Time-dependent Residual Stresses in Reinforced Concrete Columns

Castro,JTP[1*]; Vieira,RD[1]; Sousa,RA[2]; Meggiolaro,MA[1]; Freire,JLF[1]
[1]Professor, Mechanical Engineering Department, [2]MsC, Civil Engineering Department
*jtcastro@puc-rio.br, Catholic University of Rio de Janeiro, PUC-Rio,
R. Marquês de S. Vicente 225, Rio de Janeiro, RJ, 22451-900, Brazil

Abstract

Particularly careful released or alleviated strain measurements made on various steel rods of several reinforced concrete columns turn out to be much higher than initially expected. This is a critical problem, as their final objective was to evaluate the forces that were loading the columns. In fact, some loads calculated in a standard linear elastic way appear to be larger than the column's ultimate design load. However, despite its widespread use in structural design, such linear elastic calculations do not include the very significant influence of concrete creep on the columns strain, a phenomenon that is only implicitly considered by the "allowable stresses" specified in their design codes. Since this procedure is inappropriate for experimental stress analysis purposes, a relatively simple viscoelastic model is proposed to describe the concrete long term stress-strain behavior. This model is extended to model the reinforced columns, and then qualified by fitting it to concrete column creep data from the literature, proving that the measured strains are indeed compatible with the columns load history.

Introduction

A large and very busy subway station was suffering important structural modifications to serve as the main commuting point between an existing line and a new one under construction. That station was originally conceived as a crossing point. In the original plan, the new subway line would have two parallel tunnels for holding each one of its two railways, and the station was accordingly built more than ten years ago. However, its original plan had to be changed because the new line is being dug by a machine which can open holes large enough to hold the two railways inside a single tunnel. Consequently, several columns of that veteran station shall now be removed and properly replaced to allow the passage of the digging machine and the settlement of the new line with its adjacent railways. Moreover, this unusual task should be fulfilled without interrupting the old line regular transportation services. To assure the safety of this process, load measurements were specified in all the columns that will be removed or could be affected during the station upgrade.

Since direct load measurements were physically impossible in this case, because the reinforced concrete columns were built into the subway station structure, residual or resident strain measurements by localized stress releases were proposed as an alternative method for indirectly measuring the required loads (which could only be calculated from the strain measurements by using the appropriate columns stiffness properties).

The various concrete columns were approximately 1.2m in diameter. They were reinforced by some 30 or more vertical steel rods, circumferentially tied in a standardized way. The rods diameters were 16, 20 or 24mm. They had a minimum yield strain ε_{Ymin} **> 2500μm/m**, being distributed more or less circumferentially along the column perimeter. But there was no warranty about the depth of the rods, nor about the thickness of the concrete layer which covered them. This thickness, as it was later on verified, indeed varied significantly from column to column, and even around a same column.

To avoid the uncertainty associated with residual strain measurements made on concrete layers of varying thickness, small holes were opened on the columns surface to expose a small portion of some of their steel reinforcing bars. These bars were strain-gaged and then sectioned to alleviate their strains. Instead of using only three co-planar measurement points, which is the minimum number required to distinguish the normal from the bending strains, whenever possible four reinforcing bars more or less 90 degrees apart were instrumented in each column, to provide some measurement redundancy. This conservative practice is strongly recommendable, not only to avoid losing important information in case of an eventual gage problem, but also to provide some insight on the measurement dispersion. Due to the severe structural risk problem associated with the columns removal, this measurement service was made with particular care by highly trained personnel.

It is worth mentioning that the rod sectioning method could be substituted by the tick-tack-toe method proposed elsewhere [1], if the concrete layers were thick, or if the columns were made of non-reinforced concrete.

Despite all the care, the measured results turned out to be much higher than initially expected, a big problem for the engineers in charge of the expansion project. Thus, the first reaction of the experts on concrete structures, who should in principle provide the columns stiffness properties necessary for the loadings calculations, was to question the accuracy of the strain measurements. This questioning was an irrefutable and welcome challenge for the measuring team, whose solution turned out to be quite interesting, as shown in the following sections.

Measurement Details

As already mentioned, four small holes or windows were opened on the surface of most columns, spaced at approximately 90^{o} in a same transversal plane, to expose a short portion of some of their steel reinforcing bars. In a few columns, only three windows could be opened, due to access limitations, losing in this way the redundancy discussed above, but still allowing the separation of the normal from the bending loads. The windows were typically around 200mm high, and their depth and horizontal size were kept as small as possible (around 150mm wide with a 50 to 100mm depth, see Figure 1) to allow the preparation of the rod's surface for bonding the strain gage, and the subsequent cut of the lower part of the exposed rod by a 125mm abrasive wheel.

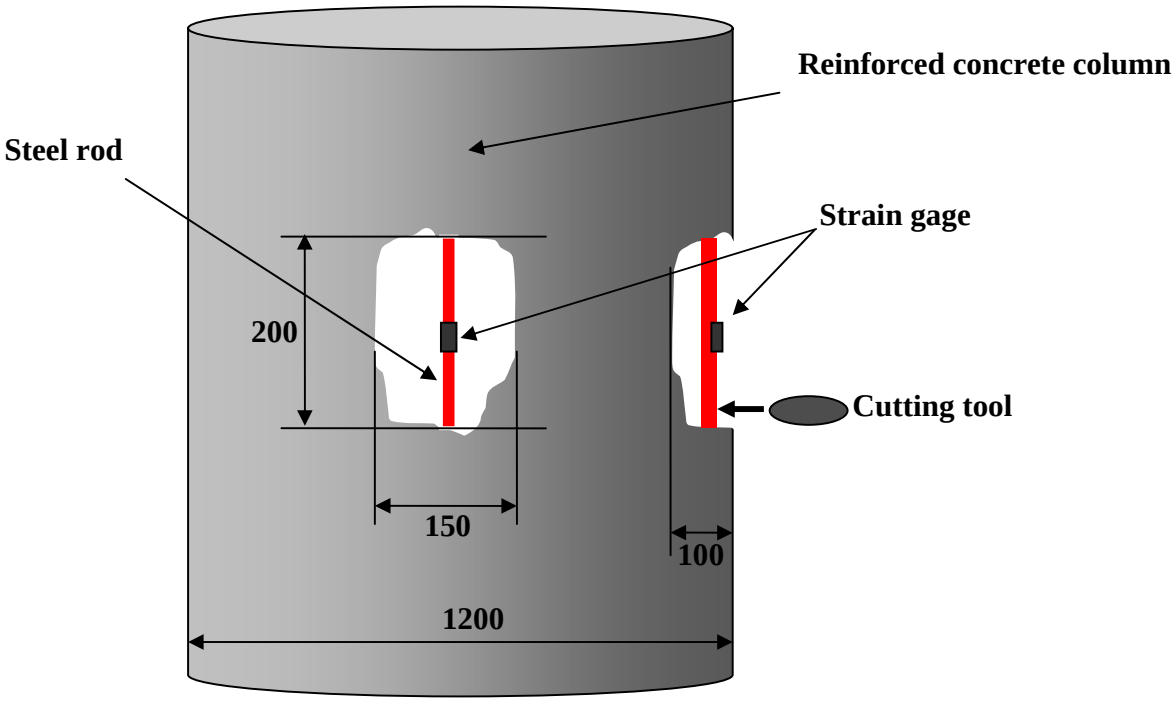

Figure 1: Sketch of the measurement procedure

A carefully grounded small plane recess was opened in the superior part of each exposed rod inside the windows. In most cases, the recess was about 8 to 12mm wide and 40 to 60mm long with a surface finished by hand using a 220 grid sand paper. A uniaxial strain gage was then bonded on this surface using a cyanoacrilate adhesive, after proper cleaning. The gages were connected to a three wire shielded cable, and then protected by a neutral silicone rubber barrier. After being bonded, cabled and protected, all the four (or three) gages of a column were connected to a precision four channel portable strain indicator, and properly balanced. Finally, the lower part of the rods were slowly cut by the abrasive wheel, always in several steps to allow proper water cooling during the progressive cutting, in order to avoid overheating the gage (what was easily achieved by holding the rods with a bare hand). The cuts were always performed at least 100mm (or more than 4 to 5 rod diameters) from the gage, and the strain readings were only made after the complete stabilization of their (small) thermal transients.

Before starting any analysis, it is important to point out that the released strain measured in any steel rod of a reinforced concrete column can in general be due to the superposition of several mechanisms, namely:

1. the rod service stress, which is caused by the column load (remembering that this load, whose evaluation is the final objective of such a measurement, generally has both a compression and a bending component);
2. concrete creep under the service load (the steel rods do not creep significantly at room temperature, but their strain also increase as time passes by to maintain their geometrical compatibility with the slowly creeping concrete);
3. concrete shrinkage during its cure (whose consequences are similar to creep);
4. residual stresses introduced during the rods' manufacturing (e.g. by non-uniform plastic deformations and/or heat treatments);
5. residual stresses introduced during the mounting of the reinforcement (by bending, torsion and/or tying of the reinforcing rods);
6. concrete removal to expose the rod for the measuring process (the load carried by that small volume is partially transferred to the exposed rod); and
7. rod cross section decrease during the preparation of its surface for bonding the gage (if the rod load is constant, its stress and strain increase as the cross section decreases).

The severance of any rod interrupts its force path and, as a result, completely releases all these strain components under the gage, no matter which mechanisms caused them. This strain alleviation can be correlated with the rod stress, and thus with the forces that were imposed in the rod to cause it, if: (i) it can be supposed that the stress caused by the load in the rod is uniaxial, a reasonable assumption in such a slender member built into a concrete column of a much larger diameter; and (ii) if all the other strain parcels can be neglected or properly evaluated.

Since the sectioning cuts where always made several rod diameters from the gages, the residual stresses eventually introduced during the rods manufacture, which are of course self-equilibrating in any cross section, should not significantly affect the gage measurements according to Saint Venant's principle. Consequently, component 4 of the above list could be safely neglected when analyzing the total released strain. As all 4 (or 3) gages of a given column were continuously monitored during the cutting process, it could be observed that cutting a rod did not influence the others, whose signals remained balanced within the strain indicator noise level (always less than $\pm 5\mu m/m$). Therefore, the column stiffness loss introduced by alleviating the instrumented rods was negligible, and so was the 6th listed component of the total rod strain. All the exposed rods were checked for lateral displacements and/or rotations after the cuts, but they maintained the alignment in almost all cases, evidence that the mounting stresses which could cause the 5th listed strain component were also negligible.

Finally, the effect of the rod cross section reduction, necessary for mounting the gage, could easily be accounted for, as schematized in Figure 2. The grinding of a short and small plane recess was needed to bond the gage (because reinforced rods have a very rough surface and a helical external thread for improving their adherence to the concrete), but they not only reduced the rod cross section but also introduced some local bending due to the eccentricity of their (assumed) pure compression load. The exposed part of the rod is really loaded under displacement control, since its strain is imposed by the rest of the column. However, since the recess was small and short, it can be modeled as if it was loaded under a pure axial load which induced a stress σ_0 on its section.

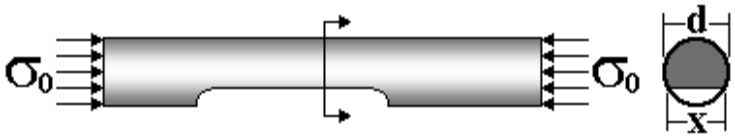

Figure 2: The small recess for bonding the gages introduces some bending strains in the rod.

Thus, if σ_0 is the pure nominal compression stress acting on the original section of a reinforcing rod of diameter **d** and area $\mathbf{A_0 = \pi d^2/4}$, **x** is the width of the recess, and $\mathbf{A = d^2(\alpha - \sin\alpha\cdot\cos\alpha)/4}$ is the area of the recess section, where $\mathbf{\alpha = \pi - asin(x/d)}$, then the stress σ under the gage (which has a normal and a bending component) is given by (see Figure 3):

$$\sigma = \frac{32\sigma_0 A_0}{3d^2}\left\{\frac{\frac{(\sin\alpha)^3}{(\alpha-\sin\alpha\cdot\cos\alpha)}\left[\frac{2(\sin\alpha)^3}{3(\alpha-\sin\alpha\cdot\cos\alpha)}-\cos\alpha\right]}{\alpha-\sin\alpha\cdot\cos\alpha+2(\sin\alpha)^3\cdot\cos\alpha-\frac{16(\sin\alpha)^6}{9(\alpha-\sin\alpha\cdot\cos\alpha)}}+\frac{1}{A}\right\} \quad (1)$$

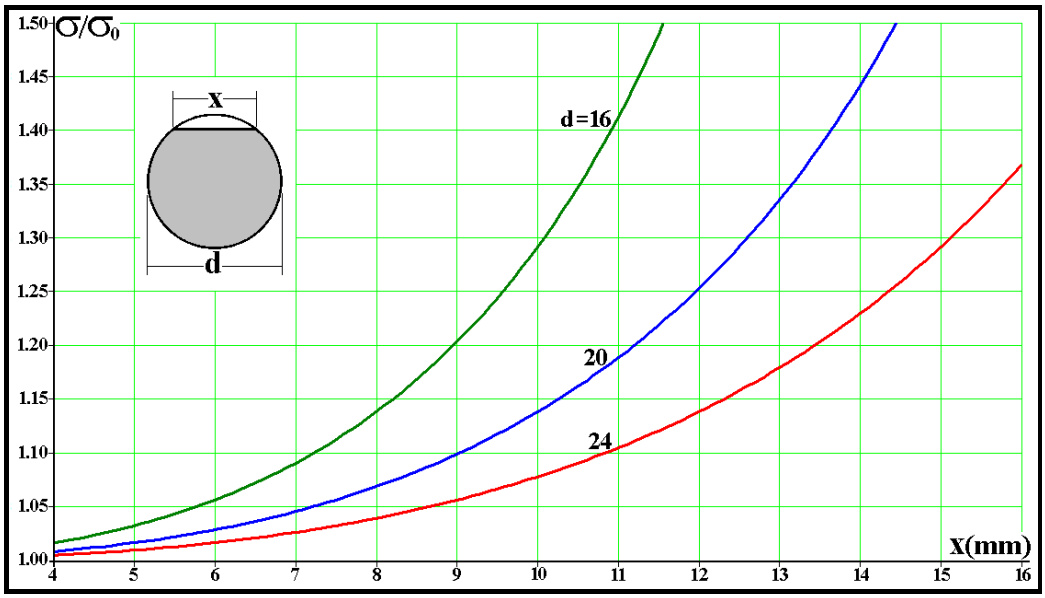

Figure 3: Ratio σ/σ_0 as a function of the recess width **x** for the three rod diameters: this effect is not negligible in most cases, and it must be accounted for in the load analysis.

The mean value of the released strains measured in more than 100 sectioned reinforcing rods of 28 columns was ε_m **= 1325μm/m**, and the maximum was ε_{max} **= 2600μm/m**. These strains are still within the linear elastic range of the steel rods, except for ε_{max} that slight above ε_{Ymin}. But they indeed seem to be too large for the concrete, whose ultimate design strain is taken as ε_U **= 2000μm/m**. No structural engineer would ever want to approach such value under the maximum load conceived for his or her design. Even after considering the recess correction, which decreased the measured strain values in average by 20%, in a first look they still would imply that the columns were or could be unsafe. But there was no other evidence of such a problem, since no cracking, screaking or any other warning was ever emitted by the columns. As a result, it was much simpler to just dismiss the measurements as wrong.

On the other hand, there was no evidence of any problem with the measured strains. The measurements followed reliable and very well established procedures, including electrical tests of the reading equipment with high precision resistors and operational tests of the installed gages, always generating consistent checks. Moreover, as the tests were made by veteran engineers with a long practical experience in the field and a sound theoretical background, their qualitative opinion is an asset that cannot be ignored. Therefore, something had to be done to make sense out of these two apparently incompatible, but very strong evidences, as explained below.

The Viscoelastic Behavior of Concrete

Concrete is made by mixing gravel, sand and a calcium silicate cement powder, which are all ceramic materials, with water, which hydrates and hardens the cement to form a rock-like composite. Therefore, it may sound strange to talk about concrete creep at room temperature. Nevertheless, concrete can creep a lot. For example, Figure 4 shows some concrete creep data presented by Leeth [2]. According to Buyukozturk [3], concrete creep is influenced by factors that can be internal, dependent on the concrete composition (such as concentration, stiffness, grading, distribution and permeability of the aggregate, water/cement ratio, cement type, etc.), or external, dependent on structural parameters (size, shape, environment, loading, etc.). Moreover, creep strains are linearly proportional to the stress if $\sigma < f'_c/2$, where f'_c is the concrete compressive strength, usually measured after a 28 day curing time.

The three curves shown in Figure 4 show only the creep strains measured under 2.1, 4.2 and 6.3MPa, which after 600 days are ε_{cr} **= 446**, **872** and **1325μm/m**, but the total strain has also an initial elastic part $\varepsilon_{el} = \sigma/E$ **= 100**, **200** and **300μm/m**, respectively. Thus, the creep strains are ***not*** negligible in these tests. Moreover, the creep strains are indeed linearly proportional to the stresses, as shown in Figure 5, where the curves obtained under 2.1 and 4.2MPa practically coincide with the 6.3MPa curve when multiplied by 3 and 1.5, respectively.

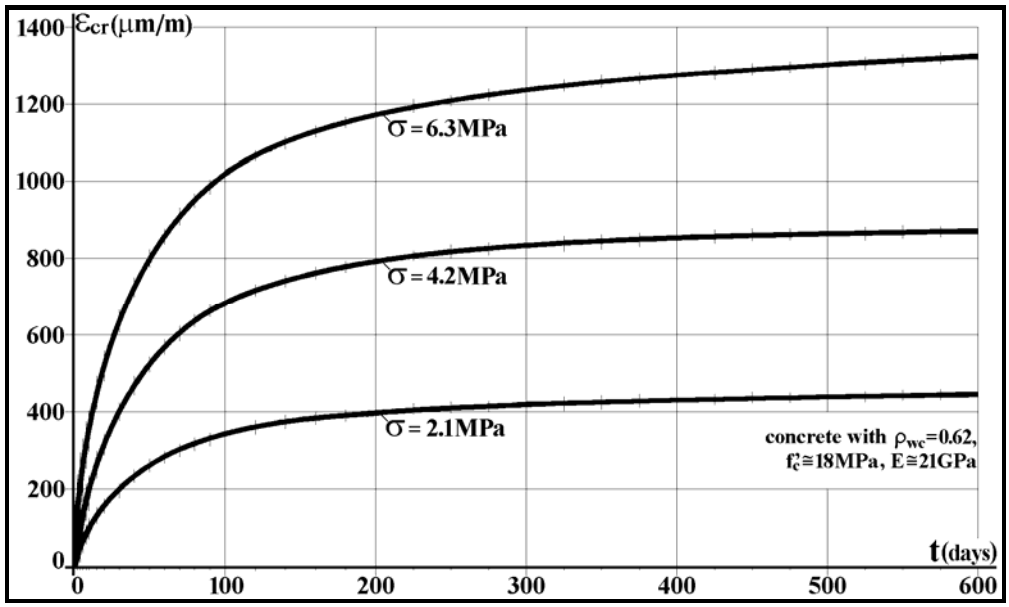

Figure 4: Time variation of creep strains under compressive stresses for a concrete with $\mathbf{f'_c = 18MPa}$ [2], Young's modulus $\mathbf{E_{c_{28}} \cong 1.36\sqrt{\rho_c^3 \cdot f'_c} \cong 21GPa}$ (both measured, as usual, 28 days after casting), water/cement ratio $\boldsymbol{\rho_{wc} = 0.62}$, and density $\boldsymbol{\rho_c \cong 2.3}$. The stresses and strains are plotted as positives for convenience.

The next step is to find a proper rheological model to reproduce all these curves, which should not include the elastic strains as they show only the creep strains. A first option could be to try to fit the data by a Kelvin-Voigt equation, but as the experimental creep data does not show a horizontal assimptote, at least another damper is needed in the model.

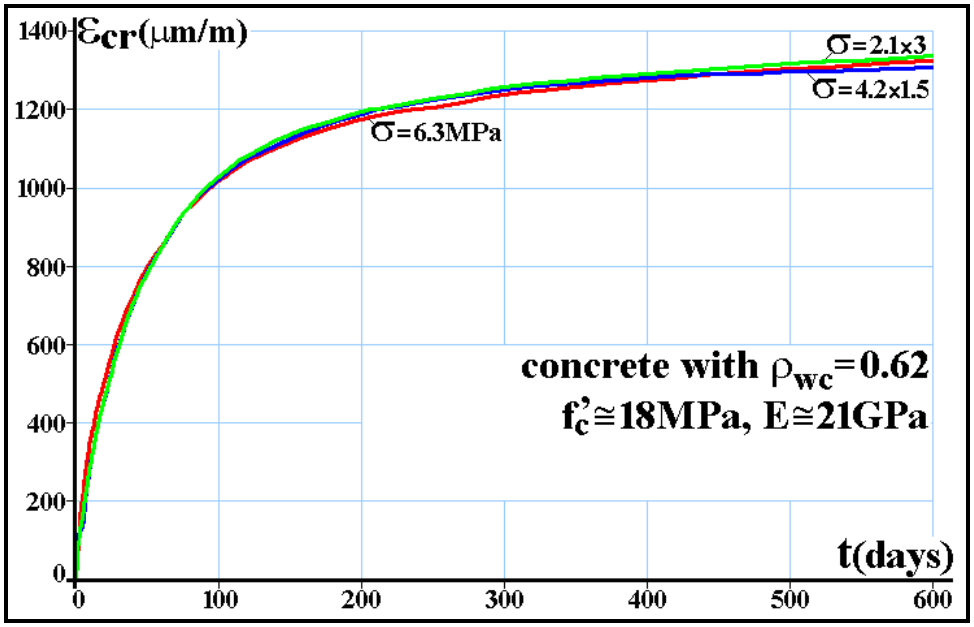

Figure 5: The concrete whose creep curves are shown in Figure 4 is indeed a linear viscoelastic material, since the 3 curves practically coincide when properly scaled by a $\mathbf{6.3/\sigma}$ factor.

A generic non-linear curve can be fitted to a set of data by minimizing its mean square deviation from that set using the Levenberg-Marquardt (LM) algorithm [4-5]: given a set of **m** points $\mathbf{(x_i, y_i)}$, $\mathbf{i = 1, \cdots, m}$, LM searches for the parameters' vector $\mathbf{p = [p_1, p_2, \cdots, p_n]^T}$ (where **T** means transpose) containing the **n** constants of the specified $\mathbf{f(x_i, p)}$ function which minimizes the sum of the square deviations:

$$S(p) = \sum_{i=1}^{m} [y_i - f(x_i, p)]^2 \tag{2}$$

LM can be applied to non-linear vectorial functions, whereas x_i can be a scalar for one-variable functions, or a vector for functions of more than one variable. But in the following formulation, $f(x_i, p)$ and y_i are supposed scalars. It is didactic to present a few examples, e.g. in fatigue: in Paris' rule $da/dN = f(x_i, p) = A_p \cdot \Delta K^{mp}$, $x_i = \Delta K$ and $p = [A_p, m_p]^T$; in Walker's rule $da/dN = f(x_i, p) = A_w \cdot \Delta K^{mw}/(1 - R)^{pw}$, $x_i = [\Delta K, R]^T$ and $p = [A_w, m_w, p_w]^T$; and in Coffin-Manson's rule $\Delta\varepsilon = f(x_i, p) = (2\sigma_c/E)(2N)^b + (2\varepsilon_c)(2N)^c$, $x_i = N$ and $p = [\sigma_c, E, b, \varepsilon_c, c]^T$.

LM is an iterative procedure, which depends on an initial estimate for the vector p, which for highly non-linear functions needs to be close to the final solution to guarantee convergence. But this normally is not necessary for fitting data obtained in mechanical tests. In each iteraction, p is replaced by a new estimate $p + q$. To find the vector $q = [q_1, q_2, \cdots, q_n]^T$, the functions $f(x_i, p + q)$ are approximated by their linearizations, given by:

$$f(x_i, p + q) \cong f(x_i, p) + J(x_i, p) \cdot q \tag{3}$$

where J is the Jacobian of f with respect to p:

$$J(x_i, p) = \left[\frac{\partial f(x_i, p)}{\partial p_1}, \frac{\partial f(x_i, p)}{\partial p_2}, \cdots, \frac{\partial f(x_i, p)}{\partial p_n} \right] \tag{4}$$

In the case discussed here, as f is scalar, the Jacobian results in the gradient of f with respect to p. When the sum of the deviations $S(p)$ is minimum, the gradient of S with respect to q is equal to zero. Therefore, applying equation (2) at $S(p + q)$, and making $\partial S/\partial q = 0$, results in:

$$\sum_{i=1}^{m} \{J(x_i, p)^T \cdot J(x_i, p)\} \cdot q = \sum_{i=1}^{m} \{J(x_i, p)^T \cdot [y_i - f(x_i, p)]\} \tag{5}$$

In this manner, the correction vector q can be obtained in each iteraction by:

$$q = \left[\sum_{i=1}^{m} J(x_i, p)^T \cdot J(x_i, p) \right]^{-1} \cdot \sum_{i=1}^{m} \{J(x_i, p)^T \cdot [y_i - f(x_i, p)]\} \tag{6}$$

All the m experimental data points can be stacked in a $m \times n$ matrix J_t and in an $m \times 1$ error vector e_t, defined as:

$$J_t(p) \equiv \begin{bmatrix} J(x_1, p) \\ J(x_2, p) \\ \vdots \\ J(x_m, p) \end{bmatrix} \quad \text{and} \quad e_t(p) \equiv \begin{bmatrix} y_1 - f(x_1, p) \\ y_2 - f(x_2, p) \\ \vdots \\ y_m - f(x_m, p) \end{bmatrix} \tag{7}$$

Then, equation (6) can be rewritten as:

$$q = (J_t^T J_t)^{-1} J_t^T \cdot e_t \equiv \text{pinv}(J_t) \cdot e_t \tag{8}$$

where $\text{pinv}(J_t)$ is known as the pseudo-inverse of J_t, with $\text{pinv}(J_t) \equiv (J_t^T J_t)^{-1} J_t^T$. After finding q in each iteraction and summing it to the current p estimate, the algorithm continues updating p until the correction q has absolute value smaller than a given tolerance.

If f varies linearly with p, then J does not depend on p, and the algorithm converges in only one iteration. Even when J depends on p, the use of a log-log scale usually guarantees convergence in a few iterations. It is advisable to monitor the value of the deviation sum $S(p)$, which should always decrease at each iteration. If $S(p)$ increases in some iteration, a possibility when working with highly non-linear functions, it is necessary to introduce a positive damping term λ in the pseudo-inverse:

$$q = (J_t^T J_t + \lambda I)^{-1} J_t^T \cdot e_t \tag{9}$$

where **I** is the identity matrix **n×n**. The damping factor λ is updated at each iteration. If the **S(p)** reduction is too high, smaller values are chosen for λ to avoid that the algorithm becomes unstable. On the other hand, if **S(p)** decreases too slowly, λ is increased to accelerate the convergence of the iterative calculations.

Marquardt [29] recommends that damping be introduced in the numerical calculation algorithm for calculating the correction vector **q** by guessing an initial value $\lambda = \lambda_0 > 0$ and a correction factor **v > 1**, e.g. $\lambda = 1$ and **v = 2**. At each iteration, **q** is calculated using a damping factor λ/v. If **S(p + q) < S(p)**, then this **q** is summed to **p**, $\lambda = \lambda/v$ is chosen as the new factor, and a new iteration is made. In the opposite case, **q** is recalculated using λ. If **S(p + q) < S(p)**, then this **q** is summed to **p**, λ is maintained, and a new iteration begins. If in both cases **S(p + q)** $\geq$ **S(p)**, then **q** is recalculated with damping factors $\lambda \cdot v^k$, **k = 1, 2, ···**, at each new iteration until obtaining **S(p + q) < S(p)**. When this occurs, then this **q** is summed to **p**, $\lambda = \lambda \cdot v^k$ is chosen as the new damping factor, and the iterations continue. With this procedure, the algorithm stability is guaranteed.

As shown in Figure 6, two viscoelastic models are used to fit the average of the curves shown in Figure 5, using the above procedures. The first model is Kelvin-Voigt's, with its 2 parameters **k** and **c** obtained by minimizing the mean square error, generating curve 1. The second is a Kelvin-Voigt model in series with a damper, generating curves 2 and 3, either by applying the same method or by visually re-fitting the parameters $\mathbf{c_1}$, $\mathbf{c_2}$ and $\mathbf{k_2}$, respectively. The introduction of a damper in series with the Kelvin-Voigt element improves the data fitting, but the "optimum" mathematical adjustment is not as good as the old-fashioned eye-ball data fitting used to obtain curve 3. This visual tuning of the parameters generated by LM is a much recommended procedure, since there is no substitute for a well trained human judgment: the eye-ball fitting does not minimize the least square error, however it ended up fitting better the long-term creep behavior, especially after 500 days. But such a refinement by man-machine interaction is only possible after knowing the mathematically optimized parameters. In these cases, it is a particularly powerful tool when working with non-linear functions.

The LM generated curve 1 parameters are **k = 5GPa** and **c = 21.6GPa·s**, whereas for curve 2 the optimum parameters are $\mathbf{c_1}$ **= 1.196TPa·s**, $\mathbf{k_2}$ **= 5.8GPa** and $\mathbf{c_2}$ **= 18.92GPa·s**. The visual adjustment of curve 3 generates $\mathbf{c_1}$ **= 1.814TPa·s**, $\mathbf{k_2}$ **= 5.8GPa** e $\mathbf{c_2}$ **= 21.6GPa·s**. But to model the total concrete strain, another spring $\mathbf{k_1}$ **= 21GPa** in series with the damper $\mathbf{c_1}$ must be used to simulate the elastic modulus $\mathbf{E_{c28}}$ estimated above, see Figure 7.

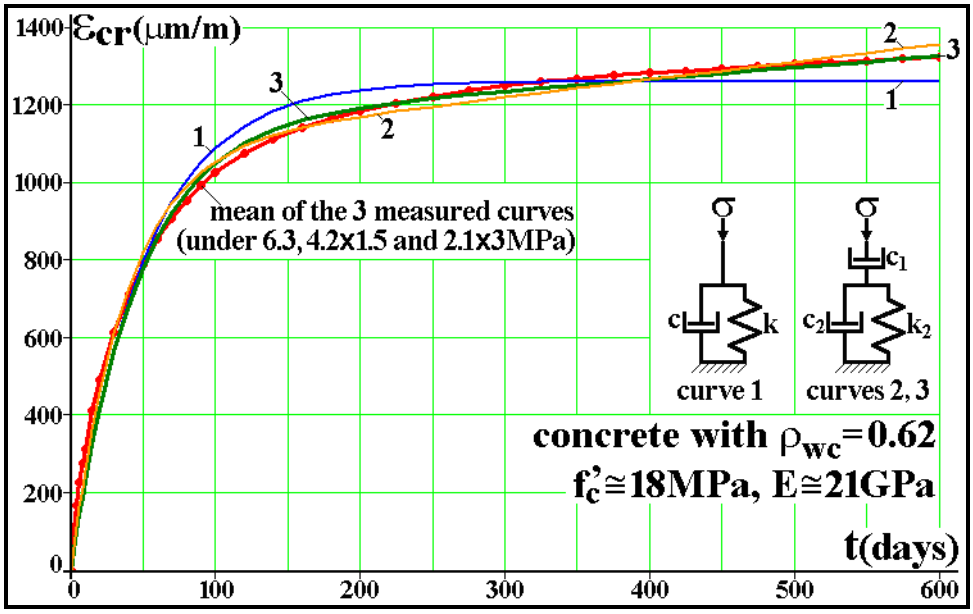

Figure 6: Fitting of Figure 5 concrete creep data.

This 4-element Burger model shown in Figure 7 is capable of reproducing well the long term mechanical behavior of the concrete whose creep data is given in Figure 4. However, to model a reinforced concrete column under pure compression, it is necessary to use still another spring in parallel with the Burgers model, to describe the effect of the steel rods. Only one spring is needed because the steel creep can be neglected at room temperature. Also, this spring is in parallel with the concrete model because both see the same strains to maintain geometric compatibility.

Therefore, if A_s is the total area of the reinforcing steel rods and A_c is the concrete area in a column whose cross section area $A = A_s + A_c$, then $fa_s = A_s/A$ and $(1 - fa_s)$ are the area fractions of the steel and the concrete in the column. If **F** is the force (supposed constant) which loads the column; E_s is the steel elastic modulus (which does not creep) and $E_c(t)$ is the (variable) creep modulus of the concrete; $\sigma_s(t)$ and $\sigma_c(t)$ are the stresses on the rods and on the concrete (both vary in time, since the concrete creep transfers loads to the steel reinforcing rods); and $\varepsilon(t)$ is the column strain (which also varies as time passes by), then it is trivial to show that the compressive force in the column is $F = \sigma_s(t)\cdot A_s + \sigma_c(t)\cdot A_c = \varepsilon(t)\cdot[E_s\cdot A_s + E_c(t)\cdot A_c]$, therefore:

$$\varepsilon(t) = \frac{F}{E_S A_S + E_C(t) A_C} = \frac{F/A}{fa_S k_S + \dfrac{(1-fa_S)}{1/k_1 + t/c_1 + [1-\exp(-k_2 t/c_2)]/k_2}} \tag{10}$$

It is also easy to show that the equivalent stress in the column is given by:

$$\sigma = F/A = \varepsilon(0)[fa_S k_S + (1-fa_S)k_1] = \varepsilon_0[fa_S k_S + (1-fa_S)k_1] \tag{11}$$

The steel area in a reinforced concrete column is typically 1 to 2% of its total area. Knowing that the (elastic) ultimate strain in reinforced concrete structural design is usually assumed as 2000μm/m, a column designed for an initial strain ε_0 **= 500μm/m** can thus be considered representative of the problems found in practice. Using this value, Figure 7 shows the strain time variations expected from a pure concrete column (with f'_c **= 18MPa** and the viscoelastic properties obtained above), and from two reinforced concrete columns, one with a steel area fraction fa_s **= 0.01** and the other with fa_s **= 0.02**.

Figure 7 demonstrates that strains in the order of ε_{max} **= 1500** to **2000μm/m** are certainly not incompatible with typical working loads applied on reinforced columns made out of the concrete whose creep strains are described by Figure 4. But this figure does not include several important details about the concrete properties, which had to be estimated in order to generate the information that supports this claim, a fact that decreases its power. However, a quite comprehensive report by Ziehl et al. [6] presents several such details, removing any doubts about the adequacy of this approach.

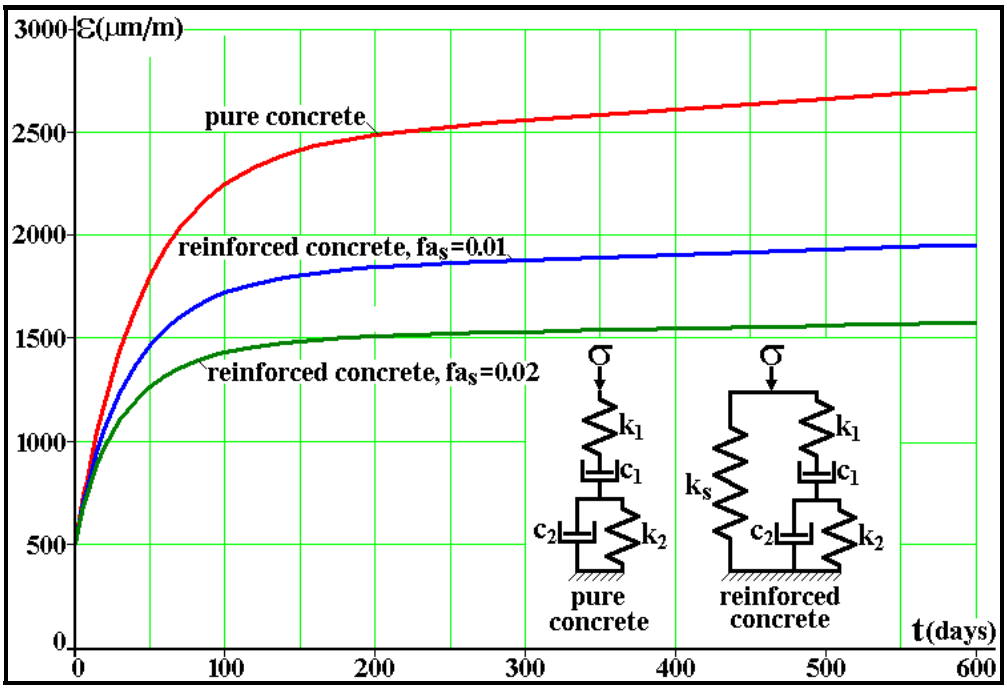

Figure 7: Strain histories $\varepsilon(t)$ estimated by equation (10) for a pure concrete and for two steel reinforced concrete columns with steel area fractions fa_s **= 1%** and fa_s **= 2%**, when they are loaded by a fixed force that causes an initial strain ε_0 **= 500μm/m**. The concrete is modeled as a linear viscoelastic Burgers' material with constant parameters k_1 **= 21GPa**, c_1 **= 1.814TPa·s**, k_2 **= 5.8GPa** e c_2 **= 21.6GPa·s**, whereas the steel reinforcement is modeled as a Hookean material with k_s **= 200GPa**.

Ziehl and his colleagues studied if reinforced concrete columns with steel area fractions $\mathbf{fa_s < 1\%}$, the minimum steel fraction required by the American standard [7-8], could be used for structural purposes. They said that those existing minimum $\mathbf{fa_s}$ requirements for columns were developed to prevent yielding of the reinforcement resulting from creep deformations in the concrete; that the tests used to support this limit were conducted decades ago, when steel yield strengths for reinforcing bars were approximately half of what is common today; and that a substantial reduction in the column steel area fraction might be possible with present-day materials, resulting in economic savings.

Ziehl et al. have cast several 203mm (8") diameter by 1219mm (4') long cylindrical columns made out of two concretes with nominal compressive strengths (at 28 days) of 28 and 56MPa (4 and 8ksi), with three steel fractions $\mathbf{fa_s}$ (0.36, 0.54, and 0.72%). They have subjected them to a constant axial load $\mathbf{F = 0.4\, f'_c\, A}$ (the maximum load allowed by ACI and AASHTO standards [7-8]) in reduced-humidity enclosures, and measured their long-term axial deformations using electronic and mechanical strain gages. The load was applied through coil springs, to provide the necessary compliance. Unloaded specimens were used to monitor temperature and shrinkage-related deformations. They presented plots of measured strain versus time, and compared the experimental results with an analytical model reported by the ACI Committee 209 [9].

The columns were cast in cardboard molds, which were stripped five days after having poured the concrete. These columns were loaded between 14 and 28 days after casting. To determine the material properties, 4×8 and 6×12 inch test cylinders were also cast for every group of columns. These cylinders were tested for modulus of elasticity and compressive strength at 7, 14, 28, and 56 days after casting. The steel rods were tested for yield and ultimate strengths. Dehumidifiers were used to keep the relative humidity and temperature generally between 30 and 60% and 10 and 43°C. The period required to load the columns for a length of time sufficient for the rate of creep to approach nearly zero was initially estimated to be close to two years, but in practice it was 15 to 18 months, depending on the specimens. Ziehl's report is particularly meticulous, and should be consulted for further details on concrete specifications and experimental procedures [6]. Figures 8-11 show how the technique discussed above can quite reasonably fit some of their data.

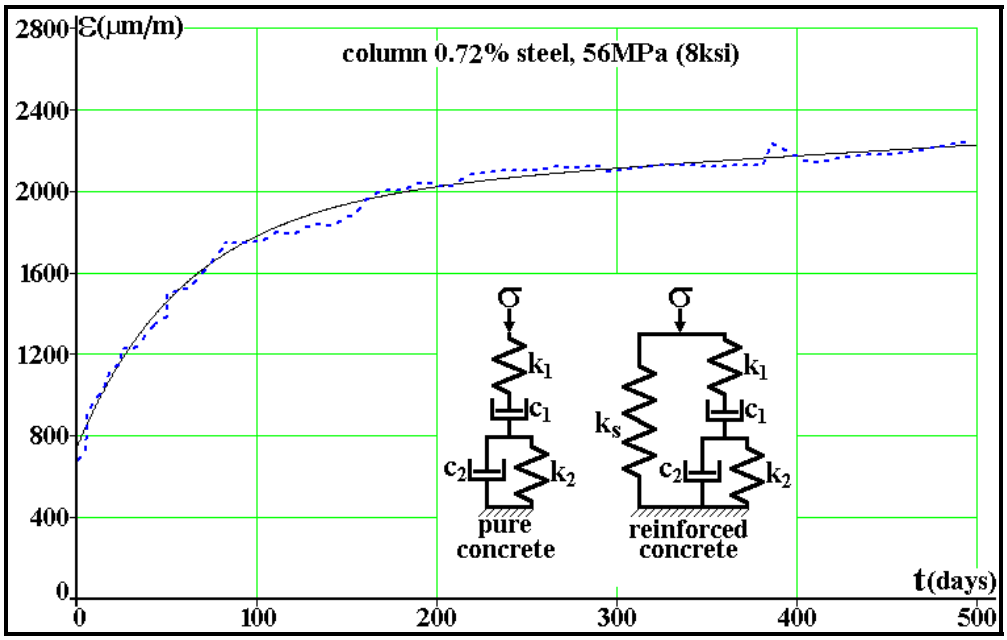

Figure 8: Total (elastic plus creep) strain history $\boldsymbol{\varepsilon(t)}$ estimated by equation (10) for a reinforced concrete column with $\mathbf{f'_c = 56MPa}$ and steel area fraction $\mathbf{fa_s = 0.72\%}$, loaded by a fixed force that induces an initial strain $\boldsymbol{\varepsilon_0 = 800\mu m/m}$: $\mathbf{k_1 = 37.54GPa}$, $\mathbf{c_1 = 40TPa{\cdot}day}$, $\mathbf{k_2 = 19GPa}$ and $\mathbf{c_2 = 1.2TPa{\cdot}day}$.

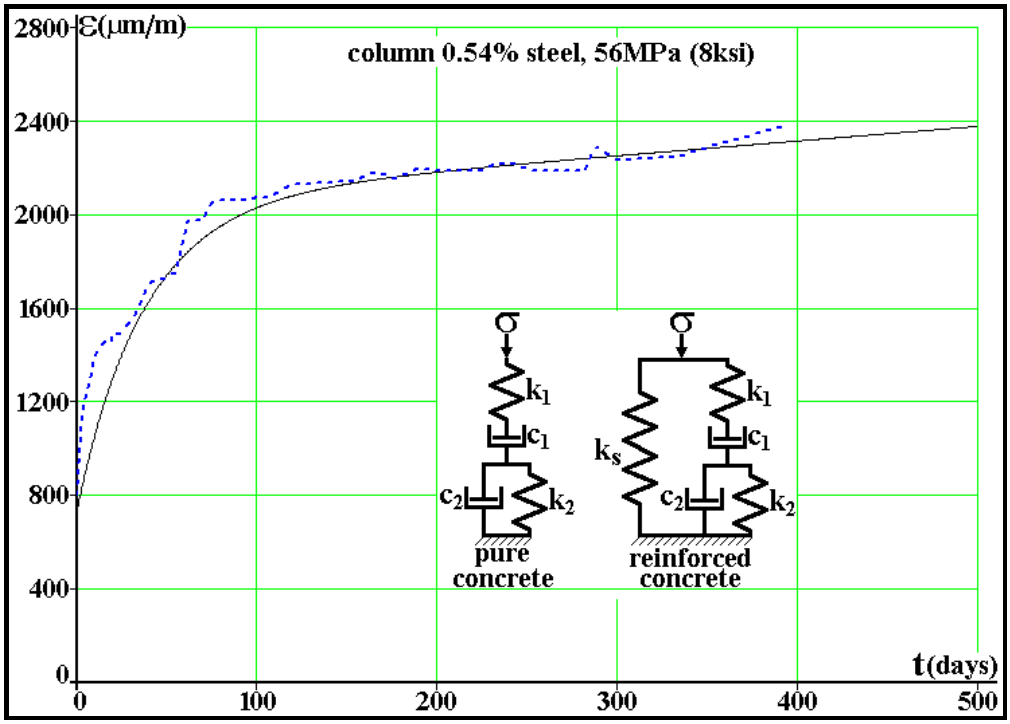

Figure 9: Total (elastic plus creep) strain history **ε(t)** estimated by equation (10) for a reinforced concrete column with f'_c **= 56MPa** and steel area fraction fa_s **= 0.54%**, loaded by a fixed force that induces an initial strain ε_0 **= 800μm/m**: k_1 **= 24.87GPa**, c_1 **= 80TPa·day**, k_2 **= 6.5GPa** and c_2 **= 340GPa·day**.

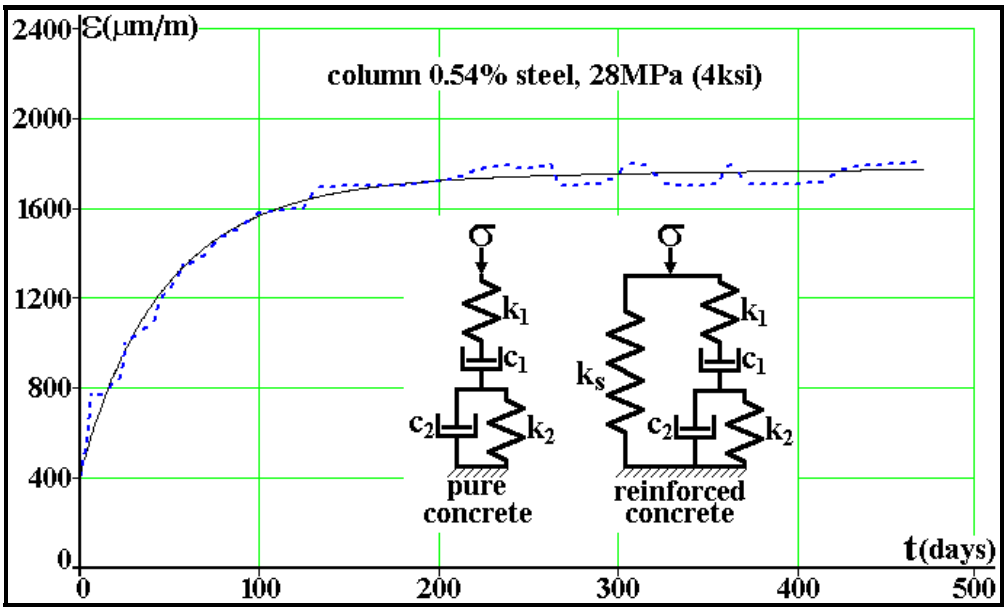

Figure 10: Total (elastic plus creep) strain history **ε(t)** estimated by equation (10) for a reinforced concrete column with f'_c **= 28MPa** and steel area fraction fa_s **= 0.54%**, loaded by a fixed force that induces an initial strain ε_0 **= 400μm/m**: k_1 **= 24.87GPa**, c_1 **= 80TPa·day**, k_2 **= 6.5GPa** and c_2 **= 340GPa·day**.

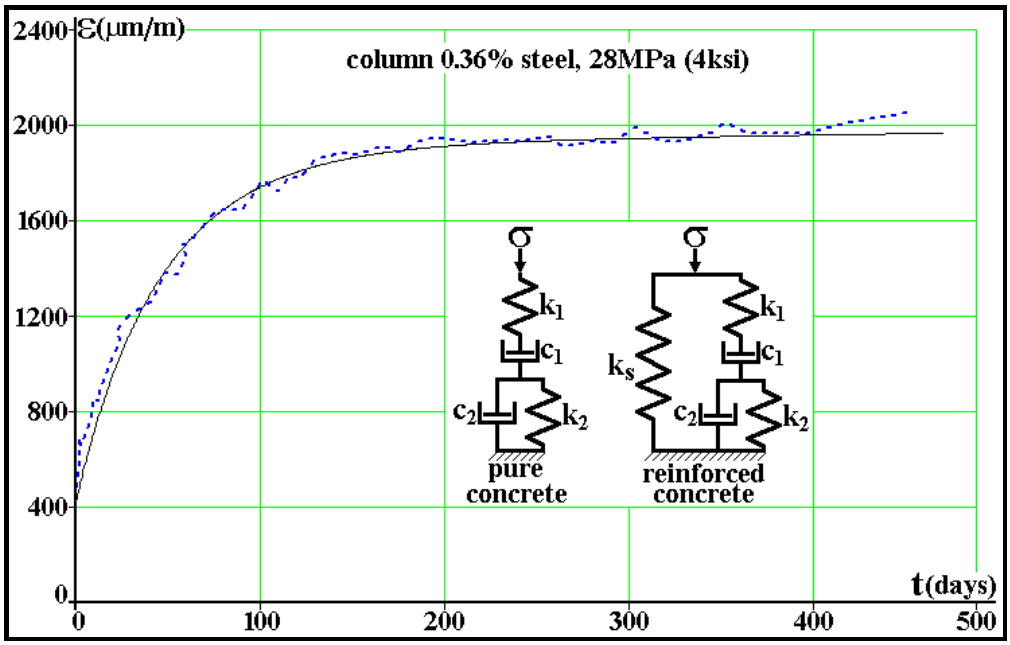

Figure 11: Total (elastic plus creep) strain history **$\varepsilon(t)$** estimated by equation (10) for a reinforced concrete column with **f'_c = 28MPa** and steel area fraction **fa_s = 0.36%**, loaded by a fixed force that induces an initial strain **ε_0 = 400μm/m**: **k_1 = 24.87GPa**, **c_1 = 70TPa·day**, **k_2 = 6GPa** and **c_2 = 300GPa·day**.

Conclusions

A relatively simple viscoelastic model was proposed to describe concrete creep, and extended to model the behavior of reinforced columns under axial loading. The model treats the concrete as a Burgers' solid, composed by a Maxwell's element with a spring **k_1** (which represents its elastic modulus) and a damper **c_1**, in series with a Kelvin-Voigt element whose spring is **k_2** and the damper is **c_2**. The reinforcing steel is modeled by a spring **k_s** in parallel with the concrete. This model satisfactorily fitted column creep data from the literature, and can be used to explain why the measured residual strains were so high when compared with the nominal design strains.

References

[1] Vieira,RD; Castro,JTP; Freire,JLF "A New Technique for Measuring Loads in Concrete Columns", Proceedings of the VI COTEQ, in CD, 2002 (in Portuguese).

[2] Leet,K. *Reinforced Concrete Design*, 2nd ed., McGraw-Hill 1982.

[3] Buyukozturk,O "Creep and Shrinkage Deformation", MIT 1.054/1.541 Mechanics and Design of Concrete Structures Course Notes, 2004.

[4] Levenberg,K "A method for the solution of certain non-linear problems in least squares", *Quarterly of Applied Mathematics* v.2, p.164-168, 1944.

[5] Marquardt,D "An algorithm for least-squares estimation of nonlinear parameters", *SIAM Journal on Applied Mathematics* v.11, p.431-441, 1963.

[6] Ziehl,PH; Cloyd,JE; Kreger,ME "Evaluation of Minimum Longitudinal Reinforcement Requirements for Reinforced Concrete Columns", Report FHWA/TX-02/1473-S, 1998.

[7] ACI Committee 318, "Building Code Requirements for Reinforced Concrete and Commentary," (ACI 318-95), ACI, Detroit, Michigan, 1995.

[8] AASHTO - American Association of State Highway and Transportation Officials, "Standard Specification for Highway Bridges," Fifteenth Edition, Washington, DC, 1992.

[9] ACI 209-R86, "Prediction of Creep, Shrinkage, and Temperature Effects in Concrete Structures," ACI, 1986.